Sensitivity analysis based on non-intrusive regression-based polynomial chaos expansion for surgical mesh modelling

Katarzyna Szepietowska · Benoit Magnain · Izabela Lubowiecka · Eric Florentin

This is the accepted version of a paper published in Structural and Multidisciplinary Optimization, DOI 10.1007/s00158-017-1799-9. The final publication is available at http://link.springer.com/article/10.1007/s00158-017-1799-9

Abstract The modelling of a system containing implants used in ventral hernia repair and human tissue suffers from many uncertainties. Thus, a probabilistic approach is needed. The goal of this study is to define an efficient numerical method to solve non-linear biomechanical models supporting the surgeon in decisions about ventral hernia repair. The model parameters are subject to substantial variability owing to, e.g., abdominal wall parameter uncertainties. Moreover, the maximum junction force, the quantity of interest which is worthy of scrutiny due to hernia recurrences, is non-smooth. A non-intrusive regression-based polynomial chaos expansion method is employed. The choice of regression points is crucial in such methods, thus we study the influence of this choice on the quantity of interest, and look for an efficient strategy. For this purpose, several aspects are studied : (i) we study the quality of the quantity of interest, i.e. accuracy of the mean and standard deviation, (ii) we perform a global sensitivity analysis using Sobol sensitivity indices. The influence of uncertainties of the chosen variables is presented. This study leads to the definition of an efficient numerical simulation dedicated to our model of implant.

Keywords Stochastic Finite Element · global sensitivity analysis · ventral hernia repair · optimal regression points choice

1 Introduction

The background of this study is ventral hernia, a common medical problem. One of the treatment methods is Laparoscopic Ventral Hernia Repair (LVHR), consisting of connecting an implant in the form of surgical mesh to the abdominal wall, under a hernia defect. Despite many medical studies on this topic, recurrences and other postoperative complications still occur [11]. There is no consensus on the material and method of fixation which should be used in incisional hernia repair [9].

In order to address this issue, a few studies have been devoted to the mechanical approach to ventral hernia problems. Junge et al. [31] investigated abdominal wall elasticity and compared it with the properties of

K. Szepietowska · I. Lubowiecka
Faculty of Civil and Environmental Engineering,
Gdańsk University of Technology, Narutowicza 11/12, 80-233 Gdańsk, Poland
E-mail: katszepi@pg.edu.pl and lubow@pg.edu.pl

B. Magnain · E. Florentin
INSA-CVL - Laboratoire PRISME
88, Boulevard Lahitolle, F-18020 Bourges, France
E-mail: benoit.magnain@insa-cvl.fr and eric.florentin@insa-cvl.fr

commercial implants. Some studies comparing mechanical behaviour of various implants were conducted by, e.g. [18] and [38]. Since it was shown that the properties of the abdominal wall are crucial in this matter [31], some studies on mechanics of the abdominal wall [55, 43] or its components, e.g. linea alba [16], were also conducted. Moreover, some physical models of the implant-abdominal wall system were performed and described in [54, 37]. Computational models of the implant-human tissue system were also developed and used in simulations [26, 35, 44].

Many uncertainties appear in modelling in ventral hernia repair context. One of the issues in mathematical modelling and design, is the high variability of the mechanical properties of the abdominal wall tissues, e.g. properties of linea alba [1] and imposed loads, e.g. the intra-abdominal pressure [15]. On the other hand, models of the human abdominal wall are often based on studies on animal *ex vivo* samples [25] due to limited data. There are only a few human studies of abdominal wall properties *in vivo* [47, 56]. Identification of human abdominal wall properties *in vivo* is challenging. In general, in the mathematical modelling of the implant-human tissue system there are a lot of uncertainties. Therefore, a probabilistic approach is required to provide information about the influence of these uncertainties on the behaviour of the implant-abdominal wall system and to include them in the implant and fixation design. As recurrences of hernia are usually caused by abdominal wall tissue-implant connection failure, the study is focused on finding for the maximum junction force, which should be minimised [36]. The second quantity of interest is maximum deflection of the implant, which is related to the issue of excessive mesh bulging. We are not only interested in distribution and statistics, but also in the sensitivity of its value with regards to the model input. Global sensitivity analysis allows the model variables to be arranged according to their impact on the variability of the output [48].

In order to solve the nonlinear Finite Element models of implant tissue systems [36], commercial software is used. Thus, a non-intrusive probabilistic method is chosen. The Monte Carlo (MC) is a very popular method [22], which allows 'black-box' models to be used. However, a large number of sampling points is required to obtain good accuracy, which in the case of more complex models can be computationally intractable. One of the methods to decrease the computational cost is polynomial chaos expansion (PC) [57]. PC is a method enabling approximation of a computational model by a series of multivariate polynomials. Ghanem and Spanos [24] developed this method in the mechanical field and proposed the spectral stochastic finite element method. Xiu and Karniadakis [59] generalized it to non-gaussian probability measures showing that convergence can be improved by employing polynomials from the Askey scheme orthogonal to the input distribution. The originally [24] proposed method of calculating coefficients - Galerkin projection - belongs to the intrusive group of methods due to code modification requirements. However, later some non-intrusive methods involving just a set of deterministic calculations without model code modification were also developed. The key methods in this group are nonintrusive projection [33] and regression method [30, 4]. Polynomial chaos expansion can also be employed to calculate global sensitivity Sobol indices [48, 17] with the computational cost hardly exceeding the case of calculating polynomial coefficients. PC can be useful in design under uncertainty in cases when a probability density function is required [34]. PC meta-models were used in reliability based design optimisation (RBDO) in [21, 49]. Moreover, the Kriging method [19] widely-used in RBDO [19] was combined with PC to create a meta-modelling methodology combining the advantages of both methods [42]. PC suffers the so-called curse of dimensionality. In order to reduce this problem an adaptive method decreasing the number of coefficients has been proposed in the literature [7].

The accuracy of meta-models created by non-intrusive PC depends on the choice of regression point. The most common approaches are to draw them randomly [14] or to choose the roots of a higher order polynomial [48]. The comparison of some methods can be found in the literature: in the context of meta-modelling and computer experiments in [13], for PC in [23] and the response surface method in [28, 58]. Nevertheless, since the efficiency of different methods is problem-dependent, it is necessary to choose carefully the regression points for a given problem with a given quantity of interest.

In this paper we apply the PC method to hernia implant modelling. The aim of the study is to compare different methods for choosing PC regression points. The goal is to find a methodology for quantification of the uncertainty in the implant tissue system models which is computationally tractable. The chosen methodology will be employed in the further study with the use of such models to optimize under uncertainty parameters of ventral hernia repair. The target models are characterized by non-linearity, non-smoothness of quantity of interest and quite a large variance of random variables.

The study is structured as follows: following the introduction, section 2 presents the surgical mesh models. In section 3 polynomial chaos expansion and the global sensitivity framework are introduced and section 4 goes on to describe different methods of choosing the regression points. We present the results of the study in section 5 which is divided into two parts: the first shows the results of the comparison of the methods for regression point choice, while the second provides the results of the global sensitivity analysis.

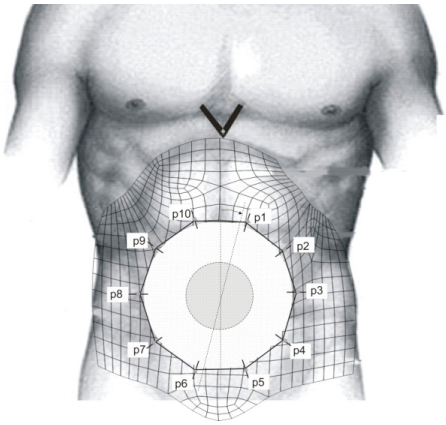

Fig. 1: Scheme of surgical mesh and abdominal wall

2 Models of the surgical mesh

We considered three models of the implant used in LVHR. The first is a simplified cable model whose results we compare with conclusions drawn on the basis of local sensitivity [51]. We also apply two Finite Element membrane models of implant (Fig. 1) with different boundary conditions. The first one is imposed on the forced displacement of supports and the second one on the intra-abdominal pressure.

2.1 Model 1: Cable model of a surgical implant

Let us consider a cable (Fig. 2) with elastic supports and displacement of the cable edges simulating an implant connected to the flexible edges of hernia [51]. The quantity of interest is the horizontal reaction H of the cable, a root of the following equation:

$$H^3(1+\frac{l_s}{L_0})+H^2(-H_0+\Delta_p\frac{EA}{L_0})-\frac{EA}{L_0}\frac{g^2l^3}{24}=0, \tag{1}$$

where E is the Young's modulus of the cable material, L_0 is the initial length of the cable, H_0 is the initial force in the cable, Δ_p the displacement of the cable edges resulting from the fascia elasticity, A the cross sectional area, g the applied pressure, l the cable span and l_s the implant overlap. The values of the constant model parameters are shown in Table 1.

Szymczak et al. [51] performed a local sensitivity analysis on this model. The identical four random variables are considered in our study $\mathbf{X}=[E,L_0,H_0,\Delta_p]^\top$. The uniformly distributed random variables are assumed with limits considered in [51]. The parameters of the distribution of the variables are presented in Table 2.

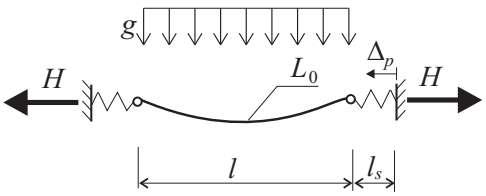

Fig. 2: Cable model

2.2 Model 2: Implant subjected to the imposed displacement of supports

The second of the surgical mesh models considered (Figure 3) refers to the case when the implant is subjected to an imposed displacement of the supports [36]. This simulates the displacement of the tacks during the deformation of the abdominal wall during daily activities [52]. This model was proposed in [36].

parameter	unit	value
A	m^2	1.35e-5
g	N/m	148.8
l	m	0.1
l_s	m	0.04

Table 1: Values of cable model parameters (1)

variable	unit	lower limit	upper limit
E	MPa	5.385	16.155
L_0	m	0.0945	0.1155
H_0	N	0	4
Δ_p	m	0.0025	0.0075

Table 2: Values of cable model random variables (1)

support	p_1	p_2	p_3	p_4	p_5	p_6	p_7	p_8	p_9	p_{10}
mean [cm]	0.575	0.2	0.225	0.4	0.45	0.45	0.4	0.225	0.2	0.575
standard deviation [cm]	0.115	0.343	0.123	0.793	0.215	0.215	0.793	0.123	0.343	0.115

Table 3: Values of mean and standard deviation of normal random variables applied as supports displacement in the implant membrane model 2

Let us consider a polygonal membrane with 10 cut corners, locating the supports where simulated fasteners are situated (Fig. 3). It is assumed that the hernia orifice has a 5 cm diameter. The mesh overlap recommended by surgeons is 4 cm. Therefore the span of the membrane is 13 cm. Fasteners are placed every 4 cm, which is the maximum distance according to the surgeon recommendations. The material model of the implant is orthotropic, piecewise linear elastic. The membrane is subjected to displacements of the supports, i.e., fastener displacement caused by the abdominal wall deformation resulting from daily activities of the patient [52]. Due to the wide variability and large uncertainty of the abdominal wall mechanical properties and consequently of the fasteners' displacement, the displacement of the supports are assumed random. The hernia is assumed to be located in the central part of the abdominal wall. The properties of one of the commercial implants (DynaMesh, properties given in[36]) are taken. The stiffer direction of the implant is assumed to be orientated vertically (parallel to the cranio-caudal axis, which is the orientation causing higher forces) for simulations done to compare methods. In the next step, the orientation is changed from 0 to 90 degrees with 15 degree steps. The random variables are assumed to be independent and normally distributed. The mean values and standard deviations are taken from [52], post-processed as in [36] and presented in Table 3.

It can be seen that some of the variables are characterized by quite a large variance (e.g. p_4).

The Finite Element system MSC Marc is used. The model is composed of 8-node quadrilateral membrane elements. The analysis is geometrically and physically non-linear.

Due to the fact that recurrences of hernia are usually caused by connection failure, our study is focused on the maximum connection force, which is also a reaction force in the model supports. The supports simulate the connection between implant and fascia. The reaction forces are calculated in each support and then a maximum of them is found in order to obtain the maximum connection force:

$$R_{max} = \max(R_i) \quad \text{for} \quad i = 1, \ldots, n_{fas}, \tag{2}$$

where R_i is the reaction force in i-th model support, and n_{fas} is the number of fasteners which is equal to the number of model supports. In the presented example, $n_{fas} = 10$. Calculating the maximum can lead to a non-smooth problem, which can be challenging for a PC method. Therefore, two approaches are proposed and compared:

Approach 1 - direct approach with one meta-model, where the quantity of interest approximated by PC is directly R_{max}:

$$Y = R_{max}; \tag{3}$$

Approach 2 - alternative approach is to firstly create a meta-model for each reaction separately:

$$Y_i = R_i \tag{4}$$

and then to find the maximum from the realisations of all meta-models at randomly chosen 10^5 sample points.

$$Y = \max(Y_i) \quad \text{for} \quad i = 1, \ldots, n_{fas}. \tag{5}$$

variable	lower limit	upper limit
p_{ia} [mmHg]	40	127
k_f [kN/m]	0.6	15.5
k_{aw} [kPa]	17	38.5

Table 4: Limit of unifrom distribution, model 3

The second approach can help in dealing with non-smoothness, but the results for the target quantity of interest are not direct. Sensitivity in the second approach is calculated as in the MC method performed using a set of meta-models.

Three cases with different numbers of random variables are considered:

- Example 2-3D three random variables $\mathbf{X} = [p_i]^\top, i = 1, 2, 3$ (other kinematic perturbations are deterministic). This example is not physically meaningful. It has been considered because of smaller computational cost and lack of the rank-deficiency problem, which appears in case of 10D problem. In this case, the calculation of the sensitivity indices by MC is expensive, but still affordable.
- Example 2-10D (all kinematic perturbations are modelled by independent random variables) $\mathbf{X} = [p_i]^\top$, $i = 1, \ldots, 10$
- Model with reduced number of variables based on sensitivity analysis outcome of 10D model.

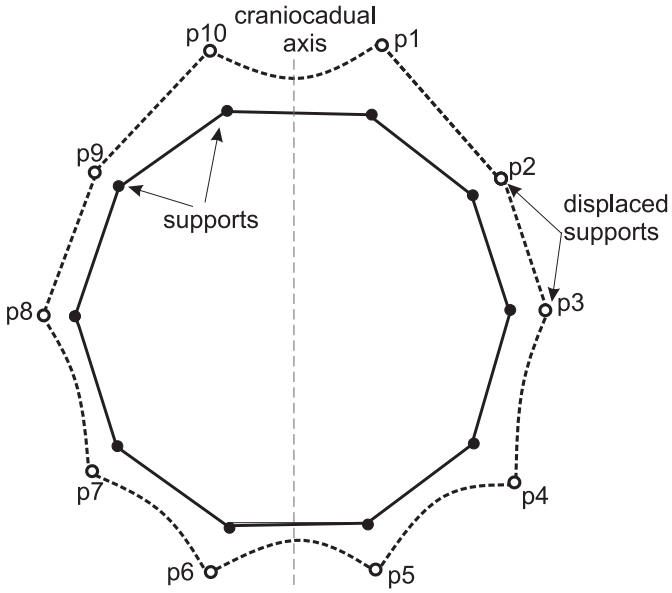

Fig. 3: Scheme of model 2 - the implant subjected to displacement of supports

2.3 Model 3: implant subjected to intra-abdominal pressure

The third model (Figure 4) is also composed of membrane elements [35]. It is subjected to dynamic pressure p_{ia} simulating intra-abdominal pressure during coughing [15]. In the overlap region of an implant with the abdominal wall there is an elastic foundation zone with elasticity k_{aw} simulating the elasticity of the abdominal wall layers. In the location of tacks elastic springs are situated with elasticity k_f relating to the fascia elasticity.

The most uncertain factors are modelled by uniformly distributed random variables (Table 4). The limits of p_{ia} are based on the study of Cobb et al. [15]. Limits of elastic foundation stifness related to the abdominal wall stiffness are based on *in vivo* study of Song et al [47] and of the spring stifness related to the fascia stiffness in [53].

In this case there are two quantities of interest: the maximum reaction of all the supports R_{max} and the maximum deflection of the center of the implant u_{max}. Since this is a dynamic analysis, the maximum over time is also found.

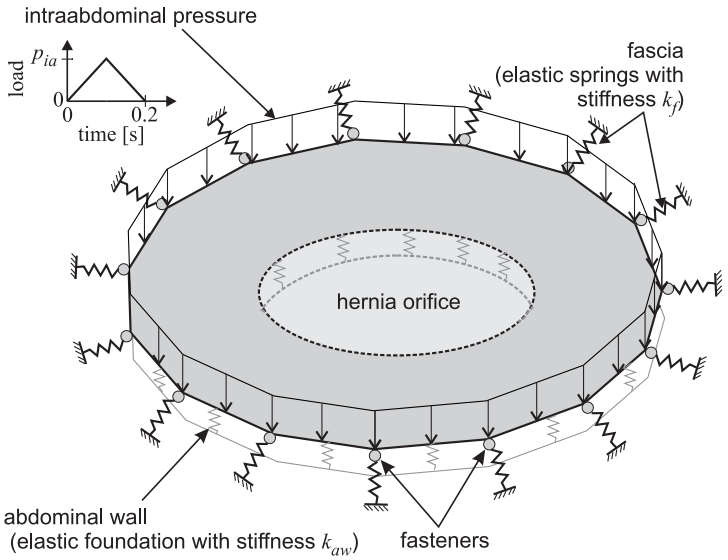

Fig. 4: Scheme of model 3

3 Polynomial chaos expansion for stochastic problems

Let $\mathcal{M}$ be the considered computational model. The model $\mathcal{M}$ is a deterministic mapping:

$$y = \mathcal{M}(\mathbf{x}), \tag{6}$$

where $\mathbf{x} = [x_1, \ldots, x_M]^\top \in \mathbb{R}^M$, with the number of variables $M \geq 1$, is an input and y is an output — the quantity of interest. Due to uncertainties, the input is represented by a random vector $\mathbf{X}(\omega)$, $\omega \in \Omega$ with joint probability density function (PDF) $f_{\mathbf{X}}$, where Ω is the space of random events ω. Hence, the model response is also a random variable:

$$Y(\omega) = \mathcal{M}(\mathbf{X}(\omega)). \tag{7}$$

For simplicity of notation ω will be skipped in the following text.

In view of potential application to arbitrarily complex models, we will only consider non-intrusive methods. In such methods, a random output is obtained by a series of deterministic calculations. Therefore, model $\mathcal{M}$ can be even discretized by the Finite Element (FE) method and the commercial FE 'black-box' system can be used to solve the problem. This makes the presented methods easily applicable.

3.1 Global sensitivity

The global sensitivity can be used to quantify the global effect of uncertain input variables on the model response.

To derive Sobol sensitivity indices [46,6], the model (6) is decomposed as follows:

$$\mathcal{M}(\mathbf{X}) = \mathcal{M}_0 + \sum_{i=1}^{M} \mathcal{M}_i(X_i) + \sum_{1 \leq i < j \leq M} \mathcal{M}_{ij}(X_i, X_j) + \cdots + \mathcal{M}_{1,2\ldots M}(\mathbf{X}). \tag{8}$$

This is called ANOVA (ANalysis Of VAriance) decomposition and is unique if:

$$\int_{\mathcal{H}_{X_k}} \mathcal{M}_{i_1 \ldots i_s}(X_{i_1}, \ldots, X_{i_s}) f_{X_k}(X_k) dX_k = 0 \quad \text{for} \quad 1 \leq i_1 < \cdots < i_s \leq M,\ k = i_1, \ldots, i_s \tag{9}$$

$$\mathcal{M}_0 = \int_{\mathcal{H}_{\mathbf{x}}} \mathcal{M}(\mathbf{X}) f_{\mathbf{X}}(\mathbf{X}) dX_i \ldots dX_M, \tag{10}$$

where $\mathcal{H}_{\mathbf{X}}$ is the support of random vector $\mathbf{X}$ and $\mathcal{H}_{X_k}$ is the support of random variable X_k, f_{X_k} is the marginal PDF of random variable X_k. All the variables $X_i, \ldots, X_M$ are independent, so $f_{\mathbf{X}}(\mathbf{X}) = \prod_{i=1}^{M} f_{X_i}(X_i)$.

In order to obtain one-dimensional terms, $\mathcal{M}_i(X_i)$, the formula (8) is integrated with respect to the probability measure over all variables except X_i over an associated domain $\mathcal{H}_{\mathbf{X}\setminus X_i}$:

$$\int\limits_{\mathcal{H}_{\mathbf{X}\setminus X_i}} \mathcal{M}(\mathbf{X}) \prod_{k\neq i} f_{X_k} dX_k = \mathcal{M}_0 + \mathcal{M}_i(X_i). \tag{11}$$

In order to obtain two-dimensional terms, $\mathcal{M}_{ij}(X_i, X_j)$, the formula (8) is integrated over all variables except x_i and x_j over an associated domain $\mathcal{H}_{\mathbf{X}\setminus\{X_i,X_j\}}$:

$$\int\limits_{\mathcal{H}_{\mathbf{X}\setminus\{X_i,X_j\}}} \mathcal{M}(\mathbf{X}) \prod_{k\neq i,j} f_{X_k} dX_k = \mathcal{M}_0 + \mathcal{M}_i(X_i) + \mathcal{M}_j(X_j) + \mathcal{M}_{i,j}(X_i, X_j) \tag{12}$$

and so on, to obtain higher dimension summands.

The partial variances are:

$$D_{i_1\ldots i_s} = \int\limits_{\mathcal{H}_{X_{i_1},\ldots,X_{i_s}}} \mathcal{M}^2_{i_1\ldots i_s}(X_{i_1}, \ldots, X_{i_s}) f_{X_{i_1,\ldots,i_s}} dX_{i_1} \ldots dX_{i_s} \tag{13}$$

and the total variance is:

$$D = \int\limits_{\mathcal{H}_{\mathbf{X}}} \mathcal{M}(\mathbf{X})^2 f_{\mathbf{X}} dX_1 \ldots dX_M - \mathcal{M}_0^2. \tag{14}$$

The global sensitivity indices are:

$$S_{i_1,\ldots,i_s} = \frac{D_{i_1,\ldots,i_s}}{D}. \tag{15}$$

The total global sensitivity index is the sum of all sensitivity indices including the mixed terms, which correspond to the i-th variable:

$$S_i^{Tot} = \sum_{i\subset\{i_1,\ldots,i_s\}} S_{i_1,\ldots,i_s}. \tag{16}$$

It can also be shown that:

$$S_i^{Tot} = 1 - S_{\sim i}, \tag{17}$$

where $S_{\sim i}$ is a sum off all partial indices which do not include the i-th variable.

3.2 Monte Carlo method

The MC method [22] is based on evaluations of the deterministic model $\mathcal{M}$ done for N_{MC} sampling points generated with a given PDF. It is one of the most popular and widely used non-intrusive methods.

Let $\mathbf{X}_n = [X_{1n}, X_{2n}, \ldots, X_{Mn}]^\top$ be n-th sample point, $n = 1, 2, \ldots N_{MC}$. The mean $\mathcal{M}_0$ can be estimated by:

$$\mathcal{M}_0 \approx \mathcal{M}_0^{MC} = \frac{1}{N_{MC}} \sum_{n=1}^{N_{MC}} \mathcal{M}(\mathbf{X}_n) \tag{18}$$

and the variance D as

$$D \approx D^{MC} = \frac{1}{N_{MC}} \sum_{n=1}^{N_{MC}} \big(\mathcal{M}(\mathbf{X}_n)\big)^2 - (\mathcal{M}_0^{MC})^2. \tag{19}$$

The $\mathcal{M}_{p\%}$ estimate percentile $p\%$, when $p\%$ of N_{MC} realisations gives the value $\mathcal{M}(\mathbf{X}_n) \leq \mathcal{M}_{p\%}$.

3.2.1 Calculating Sobol indices using the Monte Carlo method

Two sets of N_{MC} points are independently drawn and denoted with superscripts (1) and (2). Let $\widetilde{\mathbf{X}}_{in}^{(1)} = [X_{1n}^{(1)}, X_{2n}^{(1)}, \ldots, X_{(i-1)n}^{(1)}, X_{in}^{(2)}, X_{(i+1)n}^{(1)}, \ldots, X_{Mn}^{(1)}]^\top$ be sampling points from the set (1), where $X_{in}^{(1)}$ is replaced by $X_{in}^{(2)}$ from the set (2) and let $\widetilde{\mathbf{X}}_{in}^{(2)} = [X_{1n}^{(2)}, X_{2n}^{(2)}, \ldots, X_{(i-1)n}^{(2)}, X_{in}^{(1)}, X_{(i+1)n}^{(2)}, \ldots, X_{Mn}^{(2)}]^\top$ be sampling points from the set (2), where $X_{in}^{(2)}$ is replaced by $X_{in}^{(1)}$ from the set (1). The partial variance can be approximated by:

$$D_i^{MC} = \frac{1}{N_{MC}} \sum_{n=1}^{N_{MC}} \mathcal{M}(\mathbf{X}_n^{(1)}) \mathcal{M}(\widetilde{\mathbf{X}}_{in}^{(2)}) - (\mathcal{M}_0^{MC})^2. \tag{20}$$

The partial Sobol index is:

$$S_i^{MC} = \frac{D_i^{MC}}{D^{MC}}. \tag{21}$$

In order to calculate the total Sobol index without the necessity of using all the required partial indices, one can calculate:

$$D_{\sim i}^{MC} = \frac{1}{N_{MC}} \sum_{n=1}^{N_{MC}} \mathcal{M}(\mathbf{X}_n^{(1)}) \mathcal{M}(\widetilde{\mathbf{X}}_{in}^{(1)}) - (\mathcal{M}_0^{MC})^2. \tag{22}$$

Then, the calculation of the total Sobol index can be done by:

$$S_i^{Tot,MC} = 1 - \frac{D_{\sim i}^{MC}}{D^{MC}}. \tag{23}$$

3.3 Polynomial Chaos expansion

3.3.1 Polynomial Chaos basic equations

The following description of PC is based on [48,5,6]. Let the input variables X_i in $\mathbf{X}$ of the model $\mathcal{M}$ (7) be independent. Next, the output Y may be expanded via the polynomial chaos expansion as follows:

$$Y = \mathcal{M}(\mathbf{X}) = \sum_{\boldsymbol{\alpha} \in \mathbb{N}^M} a_{\boldsymbol{\alpha}} \Phi_{\boldsymbol{\alpha}}(\mathbf{X}), \tag{24}$$

where $a_{\boldsymbol{\alpha}}$ are unknown coefficients to be computed, and $\Phi_{\boldsymbol{\alpha}}$ is multivariate polynomial basis, with multi-index $\boldsymbol{\alpha} = [\alpha_1, \ldots, \alpha_M]$. Multivariate polynomials are constructed from univariate polynomials by multiplying univariate polynomials ϕ_{α_i} of order α_i:

$$\Phi_{\alpha_1,\ldots,\alpha_M}(\mathbf{X}) = \prod_{i=1}^{M} \phi_{\alpha_i}^{(i)}(X_i). \tag{25}$$

The employed polynomials are orthonormal:

$$\langle \phi_i, \phi_j \rangle = \int_{\mathcal{H}_X} \phi_i(X) \phi_j(X) f_X(X) dX = \delta_{ij}, \tag{26}$$

where δ_{ij} is Kronecker symbol equals 1 if $i = j$ and 0 otherwise.

Xiu and Karniadakis [59] proposed choosing the polynomials according to the type of distribution. It can be shown that each subset of the orthogonal polynomials in the Askey scheme has a different weighting function in the orthogonality relationship. For example, the Hermite polynomials are orthogonal with respect to Gaussian measure and Legendre polynomials with respect to uniform probability measure.

The input random variables should be transformed into reduced variables, e.g. for normal distribution to standard normal variables:

$$\mathbf{X} = \mathcal{T}(\boldsymbol{\xi}). \tag{27}$$

Next, the model response can be expressed as a function of the reduced variables

$$Y = \mathcal{M}(\mathbf{X}) = \mathcal{M} \circ \mathcal{T}(\boldsymbol{\xi}) = \sum_{\boldsymbol{\alpha} \in \mathbb{N}^M} a_{\boldsymbol{\alpha}} \Psi_{\boldsymbol{\alpha}}(\boldsymbol{\xi}). \tag{28}$$

Since $\mathbf{X}(\boldsymbol{\xi})$, for simplicity of notation, we will write in the following text $\mathcal{M}(\boldsymbol{\xi})$.

In computational practice there is a need to truncate an infinite expansion. Let $\mathcal{A}$ be a truncation set, which is a finite subset of $\mathbb{N}^M$. The classic method of truncation, applied in the paper, is to take all M-dimensional polynomials of a degree equal to or smaller than the established maximum degree p:

$$\mathcal{A}^{M,p} = \{\boldsymbol{\alpha} \in \mathbb{N}^M : \sum_{i=1}^{M} \alpha_i \leq p\}. \tag{29}$$

Then, the cardinality of the set $\mathcal{A}$ and the required number of coefficients is $P = |\mathcal{A}^{M,p}| = \frac{(M+p)!}{M!p!}$. However, this method can be computationally intractable in the case of high-dimensional problems. In order to reduce the so-called curse of dimensionality problem one of adaptive sparse PC algorithms [5,27] can be used.

Finally, a meta-model $\mathcal{M}^{PC}$ is obtained and the response can be approximated as:

$$Y \approx Y^{PC} = \mathcal{M}^{PC}(\boldsymbol{\xi}) = \sum_{\boldsymbol{\alpha} \in \mathcal{A}} a_{\boldsymbol{\alpha}} \Psi_{\boldsymbol{\alpha}}(\boldsymbol{\xi}). \tag{30}$$

3.3.2 Computation of the coefficients

The method of computing response coefficients first used in spectral stochastic Finite Element analysis [24] requires implementation in the FE code. Hence, it can be classified as an intrusive method. In contrast, non-intrusive methods allow the black-box models, e.g. FE commercial codes. In this work only non-intrusive methods will be considered owing to the feasibility of their application to quite complex biomechanical models. However, this method depends on the choice of sampling points used in the computation. The two main non-intrusive methods for calculating coefficients are: non-intrusive spectral projection (NISP) [33] and regression approach [4]. NISP is based on orthogonal projection. The Smolyak quadrature can be employed to reduce computational cost. However, its accuracy depends on the function smoothness [17]. Huberts et al. [29] compared both approaches and concluded that regression based approach generally yields better results when compared to NISP. One of the indicated reasons was the limitations of the Smolyak quadrature. In this study we employ the regression-based approach which is less sensitive to non-smoothness.

Let the response of the model be expressed as a sum of a truncated series and a residual:

$$Y = \mathcal{M}(\mathbf{X}) = \sum_{\boldsymbol{\alpha} \in \mathcal{A}} a_{\boldsymbol{\alpha}} \Psi_{\boldsymbol{\alpha}}(\boldsymbol{\xi}) + \varepsilon. \tag{31}$$

To conduct regression, a numerical experiment must be designed. N regression points are chosen in the space of reduced variables (e.g. in the case of normal distribution standard normal space) $\Xi = [\boldsymbol{\xi}^{(1)}, \ldots, \boldsymbol{\xi}^{(N)}]$ and these constitute the so-called experimental design. The model $\mathcal{M}$ is computed on N regression points after their isoprobabilistic transformation to obtain a vector of exact solutions $Y_{ex} = [\mathcal{M}(\mathbf{X}^{(1)}), \ldots, \mathcal{M}(\mathbf{X}^{(N)})]^\top$. Let us collect the coefficients $a_{\boldsymbol{\alpha}}$ into a vector $\mathbf{a} = [a_{\boldsymbol{\alpha}_0}, \ldots, a_{\boldsymbol{\alpha}_{P-1}}]^\top$, where P is cardinality of the truncation set: $P = |\mathcal{A}|$. Let $A_{ij} = \Psi_{\boldsymbol{\alpha}_j}(\boldsymbol{\xi}^{(i)})$, $i = 1, \ldots, N$; $j = 1, \ldots, P$. Coefficients $\mathbf{a}$ can be computed by solving the least square problem minimizing ε:

$$\mathbf{a} = \left(\mathbf{A}^\top \mathbf{A}\right)^{-1} \mathbf{A}^\top Y_{ex}. \tag{32}$$

The matrix $\mathbf{A}^\top \mathbf{A}$ can be called an information matrix and $(\mathbf{A}^\top \mathbf{A})^{-1}$ is a dispersion matrix, e.g. after [2]. The elements on the main diagonal of the dispersion matrix represent variance and the others are their covariance.

3.3.3 Post-processing of coefficients and global sensitivity with PC

Applying (30) as a meta-model, the calculations even for a large number of sampling points can be conducted with a negligible computational cost to obtain the sought values or to draw output histograms. However, some values, e.g. the mean $\mathcal{M}_0$ and the variance D, can be approximated directly from the PC coefficient:

$$\mathcal{M}_0 \approx \mathcal{M}_0^{PC} = a_{\mathbf{0}}, \tag{33}$$

$$D \approx D^{PC} = \sum_{\boldsymbol{\alpha} \in \mathcal{A} \setminus \{\mathbf{0}\}} a_{\boldsymbol{\alpha}}^2. \tag{34}$$

Sobol indices can be also calculated on the basis of PC coefficients as shown by [48,6,17]. Such postprocessing of PC coefficients shows negligible computational costs, thus an entire method is very attractive when compared to MC calculations.

Let $\mathcal{A}_{i_1,...,i_s}$ be a set of $\boldsymbol{\alpha}$-tuples, such that it corresponds to the polynomials $\Psi_{\boldsymbol{\alpha}}$ which depend only on the input parameters $X_{i_1}, ..., X_{i_s}$.

$$\mathcal{A}_{i_1,..,i_s} = \{\boldsymbol{\alpha} \in \mathcal{A} : \alpha_k = 0 \Leftrightarrow k \notin \{i_1, \ldots, i_s\}\}. \tag{35}$$

Next, the truncated polynomial chaos expansion can be represented as:

$$\begin{aligned}\mathcal{M}^{PC}(\boldsymbol{\xi}) = a_0 + \sum_{i=1}^{M} \sum_{\boldsymbol{\alpha} \in \mathcal{A}_i} a_{\boldsymbol{\alpha}} \Psi_{\boldsymbol{\alpha}}(\xi_i) + \sum_{1 \le i_1 < i_2 \le M} \sum_{\boldsymbol{\alpha} \in \mathcal{A}_{i_1,i_2}} a_{\boldsymbol{\alpha}} \Psi_{\boldsymbol{\alpha}}(\xi_{i_1}, \xi_{i_2}) + ..+ \\ + \sum_{1 \le i_1 < ... < i_s \le M} \sum_{\boldsymbol{\alpha} \in \mathcal{A}_{i_1,...,i_s}} a_{\boldsymbol{\alpha}} \Psi_{\boldsymbol{\alpha}}(\xi_{i_1}, ..., \xi_{i_s}) + ... + \sum_{\boldsymbol{\alpha} \in \mathcal{A}_{1,...,M}} a_{\boldsymbol{\alpha}} \Psi_{\boldsymbol{\alpha}}(\boldsymbol{\xi}).\end{aligned} \tag{36}$$

When the employed PC basis is orthonormal, the properties (9) and (10) are fulfilled. Hence, the summands in (36) can be identified as summands in (8):

$$\mathcal{M}_{i_1,..,i_s}(\xi_{i_1}, ..., \xi_{i_s}) = \sum_{\boldsymbol{\alpha} \in \mathcal{A}_{i_1,...,i_s}} a_{\boldsymbol{\alpha}} \Psi_{\boldsymbol{\alpha}}(\xi_{i_s}, ..., \xi_{i_s}). \tag{37}$$

Next, the sensitivity indices $S^{PC}_{i_1,..,i_s}$ can be calculated as:

$$S^{PC}_{i_1,..,i_s} = \frac{1}{D^{PC}} \sum_{\boldsymbol{\alpha} \in \mathcal{A}_{i_1,...,i_s}} a^2_{\boldsymbol{\alpha}}. \tag{38}$$

Let us define the set $\mathcal{A}^{Tot}_i$ which contains all $\boldsymbol{\alpha}$-tuples containing the non-zero i-th index:

$$\mathcal{A}^{Tot}_i = \{\boldsymbol{\alpha} \in \mathcal{A} : \alpha_i > 0\}. \tag{39}$$

Then, the total sensitivity indices can be calculated as:

$$S^{Tot,PC}_i = \frac{1}{D^{PC}} \sum_{\boldsymbol{\alpha} \in \mathcal{A}^{Tot}_i} a^2_{\boldsymbol{\alpha}}. \tag{40}$$

4 Choice of regression points for PC coefficients calculation

The key problem of applying the non-intrusive polynomial chaos expansion method is the choice of points used to calculate PC coefficients. A right balance between accuracy of the quantity of interest and affordable computational cost is not easy to achieve. Many approaches have been proposed in the literature. This study focuses on two common families of methods: on the one hand random and on the other hand quasi-random methods, and deterministic methods based on optimality criteria.

4.1 Random and quasi-random choice

A widely-used method is to choose regression points through the use of random or quasi-random methods.

- Pure random sampling - a simple and widely-used method to randomly draw points with respect to the distribution.
- Latin Hypercube Sampling (LHS) [39] - also a widely-used method of choosing sampling points in the PC applications, e.g. [14]. Sample points drawn by the Latin Hypercube Sampling method are better distributed in the sample space compared to the pure random method. The method is to firstly divide PDF into N_{LHS} disjoint intervals of equal probability and then to randomly draw from each subset one value. Next the samples are permuted to obtain points in M-th space.
- Low discrepancy sequences - [40] try to maximize the uniformity of sample points. Halton and Sobol sequences are a popular choice in the literature, and are thus considered in the paper. The quasi-random methods were used in PC application in [8] and [23].

4.2 Experiment Design based on optimality criteria

Isukapalli [30] proposed the construction of the polynomial chaos numerical experiment on the roots of orthogonal polynomials. In a one dimensional case, Hermite polynomial roots fulfil D-optimal criteria taken from the theory of optimum experiment design [20]. Although problems of physical experiment design differ from computational experiments since observations are subjected to random errors, e.g. due to measurement accuracy, the same criteria have been used in the choice of PC regression points. The criterion which is the most commonly used in PC is D-optimality, e.g. [60], which is also used in response surface methodology [41]. However, as mentioned in [32], other criteria like A, E or G-optimality, may be considered in the PC application.

The D-optimal criterion was originally proposed by Smith [45]. D-optimal experimental design points $\Xi^* = [\boldsymbol{\xi}^{(1)*}, \ldots, \boldsymbol{\xi}^{(N)*}]$ leads to the minimisation of dispersion matrix $(\mathbf{A}^\top \mathbf{A})^{-1}$ determinants, which is equivalent to the maximisation of the information matrix $\mathbf{A}^\top \mathbf{A}$ determinant.

$$\det(\mathbf{A}^{*\top} \mathbf{A}^*) = \max_{\Xi}((\det(\mathbf{A}^\top \mathbf{A})), \tag{41}$$

where $\boldsymbol{A}^*_{ij} = \Psi_{\boldsymbol{\alpha}_j}(\boldsymbol{\xi}^{(i)*})$, $i = 1, \ldots, N$; $j = 1, \ldots, P$.

According to [2], the higher the determinant of the information matrix, the closer to orthogonality in the dispersion matrix. Orthogonality implies mutual independence of coefficients, which is beneficial when studying the significance of model coefficients.

It should be mentioned that the roots of a higher order polynomial $(p + 1)$ are D-optimal in the case of 1D Hermite polynomials when a weight function in the form of $w = \exp(-x^2)$ is applied. Thus, the final information matrix is in the form $\mathbf{A}^\top \mathbf{W}\mathbf{A}$, where $\mathbf{W}$ is a diagonal matrix, whose elements are w [3].

4.2.1 Multi variable experimental design

Berveiller et al. [4] used a method based on the approach proposed by Isukapalli [30] to obtain an M-dimensional input comprising combinations of Hermite polynomial roots of order $p + 1$. However, the number of $(p + 1)^M$ regression points is usually computationally intractable in engineering practice. Moreover, acceptable accuracy can usually be achieved for a much smaller number of points. Therefore, in the method mentioned, a smaller number of points is used in calculations. These points are the closest to the origin (Fig. 5a). Different recommendations about the sufficient number of points can be found in the literature, e.g. $P(M - 1)$ points [4] or $2(P + 1)$ points [30]. The main drawback of this approach compared to random-based approaches is that we can easily obtain rank-deficient information matrix [48] which requires adding more regression points.

Although the cited approach is based on the D-optimal concept, the obtained solutions are not precisely D-optimal. The D-optimal set chosen from the initial candidate set of points constructed from combinations of polynomial roots of order $p+1$ is shown in Fig.5, in contrast to the classic (points closest to the origin) approach. The D-optimal design with Hermite roots as the candidates set in the context of PC was proposed by [60]. The difference between D-optimal design including weight is visible (Figs. 5b and 5c). However, if we enlarge the candidate set we may not obtain Hermite roots, e.g. Fig. 6.

Applying sets of roots of polynomials of $p + 1$ order has also been used with uniform distribution, and in that case the Legendre polynomials are used [48]. However, in the 1D case the D-optimal solution for Legendre polynomials is the roots of $(1 - x^2)L'_p(x)$ [3], where L_p is Legendre polynomial of order p.

In [60], combinations of 1D optimal points are chosen to be the candidate set of points to the D-optimality procedure. Burnaev et al. [10] propose a uniform grid and LHS sampling in the case of the normal distribution in their method. The paper studies the influence of the choice of the initial candidate set of points from which an optimum experiment design is sought. One of the proposed methods is to choose the D-optimal set from a purely random set drawn from the distribution or from LHS sampling. Including the weight by maximizing the determinant of $\mathbf{A}^\top \mathbf{W}\mathbf{A}$ or not including it by maximizing the determinant of $\mathbf{A}^\top \mathbf{A}$, influences the optimisation outcome in the case of non-uniform distribution in D-optimality procedure. Therefore, the influence of including weight has been investigated. Figure 7 shows the difference in the optimisation outcome in these two approaches, when the candidate set of points was drawn by the LHS method. The subsequent approach is to draw at random points from a set of combinations of the 1D D-optimal points, which is similar to the classic approach but helps to avoid the rank-deficiency problem.

To sum up, the following methods are compared within this article:

S1 - Sobol sequence [8];
S2 - Halton sequence [8];

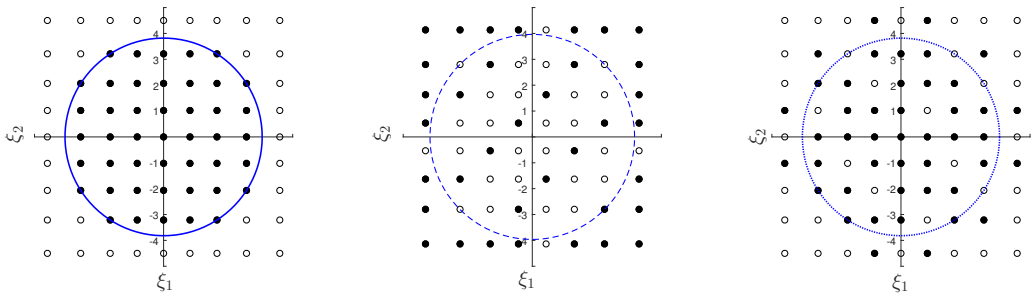

(a) Points chosen by method M1 proposed by [4]

(b) points chosen by method M2a - D-Optimal choice from candidate points set composed of the combination of polynomial roots of order $p+1$ without weight

(c) points chosen by method M2a - D-Optimal choice from candidate points set composed of the combination of polynomial roots of order $p+1$ with weight

Fig. 5: Choice of points in the case of Hermite basis, $M = 2$, $p = 7$, black points - chosen points from combinations of polynomial roots of order $p+1$

M1 - combination of roots of polynomial of order $p+1$- the closest to the origin points, classic method [48]; However, in the case of Legendre polynomials these points are not D-optimal. That is why method M1b with combination of D-optimal points in the case of uniform distribution is also investigated;

M2 - D-optimal roots from Hermite polynomial (1D - D-optimal points). In the case of normal distribution in variants:
- without weight - M2a [60];
- with weight - M2b;

M3 - randomly drawn subset of 1D - D-optimal points;

M4 - D-optimal design with a random candidate set of points. In the case of normal distribution in variants:
- without weight - M4a ;
- with weight - M4b;

M5 - D-optimal design with a candidate set sample by LHS method. In the case of normal distribution in variants:
- without weight - M5a [10];
- with weight - M5b.

In order to find the D-optimal set in the case of methods M2, M4 and M5 the row-exchange algorithm of function *candexch* build in Statistics and Machine Learning Toolbox in MATLAB 2016a is used .

5 Results

5.1 Comparison of regression point methods

The accuracy of PC for different choices of design of experiment was investigated. The methods to choose the points described in section 4 were compared on models described in section 2. The comparison of the methods is focused on the closeness of the approximated by PC meta-model solution V^{PC} to the reference value V^{ref}, which may be the mean, standard deviation, 95th percentile or sensitivity indices. The reference error $Err_{\%}$ can be defined as:

$$Err_{\%} = \frac{|V^{ref} - V^{PC}|}{|V^{ref}|} \cdot 100. \tag{42}$$

In order to compare globally the sensitivity analysis accuracy, Err_s is defined as follows:

$$Err_s = \sqrt{\sum_{i=1}^{M} (S_i^{Tot,ref} - S_i^{Tot,PC})^2}, \tag{43}$$

where $S_i^{Tot,ref}$ is a reference value of i-th random variable, obtained by MC.

It is important to remark that we only study the error due to the PC approximation. The error due to the FE approximation in example 2 is fixed and is not studied here. See, e.g. [12] for more explanations on splitting goal-oriented error estimates.

The V^{ref} is obtained by MC conducted with the use of at least 10^5 sampling points. However, performing MC for each problem is often intractable computationally. The goal of comparison of methods on model 2 is to establish a methodology which can be applied to similar models without the necessity of performing MC simulations. Since model 3 is more computationally expensive than model 2, a full MC was not performed in this case.

As a substitute for the reference solution, error estimation techniques can be used, see for example [12]. A leave-one-out method, already employed in the adaptive regression-based PC [7], can also be considered.

5.1.1 Cable model

Figure 8 shows the value of Err_s for all methods employed in model 1. It should be noted that the distance is calculated to the value already approximated by MC $S_i^{Tot,Ref} = S_i^{Tot,MC}$. Taking a combination of roots of polynomial order $p+1$ as the candidate set to D-optimisation gives a better result than the combination of 1D-D optimal points. The Halton sequence gives better results than the Sobol sequence.

5.1.2 Membrane model subjected to the displacement of supports -3D case

Firstly, the same methods are compared on the membrane example with 3 random variables (example 2-3D). The total sensitivity index S_3^{Tot} was omitted due to its very small (0.0009) value when compared to S_1^{Tot} and S_2^{Tot}.

The method M1, popular in the literature, has been tested for different orders. Figure 9 presents $Err_{\%}$ of the mean, standard deviation and 95th percentile of R_{max} obtained by: approach 1 (4) and approach 2 (5). The difference between these two approaches is not important in this example. A higher difference can be seen in the case of Err_s (Fig. 10), where for some low orders the approach 1 gives more accurate results than the approach 2. In further simulations of other examples, only approach 1 (4) is employed. Both figures represent the case when all combinations of Hermite roots of order $p+1$ are taken into account, which is more than the number of points $(M-1)P$ recommended in the literature [4] .

Figures 11 and 12 show the results obtained by method S2 for different orders and numbers of points $c \cdot P$ proportional to size of PC basis P. It can be noted that in the case of the S2 method, an increasing order may lead to an increase in error. What is more, the order which minimizes error is different for different quantities (mean, standard deviation, 95th percentile). Higher orders are more accurate for calculating the 95th percentile. As already observed in the literature, starting from a certain level, a further increase of the number of points does not significantly improve the accuracy [4] in the case of mean, standard deviation and 95th percentile. The same can be also observed in the case of Err_s for low orders of PC, but when the higher-orders are applied, the situation is less stable. These results show that it is not simple to master PC. Increasing the order of the PC is not a systematic solution for having good results. First, the computational cost increases, and the choice of points appears. Moreover, the quality of the solution may deteriorate numerically.

The methods M2, M4 and M5 were applied in two variants: not-including weight (a) and including $w = \frac{1}{\sqrt{2\pi}} e^{-\boldsymbol{\xi^2/2}}$. The calculations were performed for the same initial candidate set of points for M2a and M2b, M4a and M4b, M5a and M5b. Table 5 shows a comparison between the results obtained for both approaches for PC order 3. In the method M1, only the error of the 95th percentile is smaller in the variant without weight. Methods M4 and M5 from the point of view of the mean from repeated performance are better in the variant with weight. Moreover, in the majority of cases, including the weight leads to higher accuracy. This is also true in the case of a single pair of calculations taken from the same set performed for the same candidate set. Nevertheless, cases when some of the $Err_{\%}$ are lower without the weight can be found for some random draws and quantities.

Figures 13, 14, 15 show the error obtained using methods M2 and M5, respectively, also for higher orders. The relation between variants with and without weight can differ with the order of PC. Including the weight seems to be a better choice, when a low PC order is applied.

A comparison of all methods for example 2-3D is presented in Table 5. The sensitivity of variable number 2 is already small (0.144) so the value of the relative error seems to be high. The Halton sequence (S2) out-performs Sobol sequence (S1) in the case of all investigated quantities as observed in previous examples. To sum up, in the case of example 2-3D, method M1 is the least convenient due to rank deficiency problem (requires a larger number of regression points). The D-optimal choice seems to work in both variants, but is generally better when weight is included. That is why in the example with 10 random variables (example 2-10D) the variants without weight in method M4 and M5 were excluded due to the size of the problem. Variability of results in case of methods involving random sampling was low, especially in the case of M3.

	$Err_{\%}$					Err_s
	Mean	Standard deviation	95th percentile	S_1^{Tot}	S_2^{Tot}	
S1	0.63	30.21	3.1	9.09	82.53	0.1416
S2	0.09	20.36	0.93	7.62	49.02	0.1037
M1	4.14	11.19	0.19	5.68	75.07	0.1208
M2a	1.36	16.55	3.84	2.22	49.31	0.0742
M2b	0.96	13.19	3.29	0.21	24.65	0.0357
M3	1.43	17.82	3.96	1.59	42.42	0.0636
M4a	6.42	12.84	5.58	41.12	174.26	0.47
M4b	0.23	1.66	2.17	2.07	25.09	0.04
M5a	1.49	8.08	3.84	18.16	67.24	0.2
M5b	0.16	2.39	2.14	1.4	30	0.05

Table 5: Errors example 2-3D, $p = 3$, 40 points ($2P$). Calculations for method M1 due to rank deficiency problem were done for 49 points

.

order	1	2	3	4
P	11	66	296	1001
$(M-1)P$	99	594	2574	9009
number of points	258	147	7674	12693

Table 6: Number of regression points chosen by method M1 for $M = 10$ and Hermite basis which leads to non-rank-deficient problem compared to PC basis size P and recommended number of points $(M-1)P$

method	Mean	Standard deviation	95th percentile	S_4^{Tot}
S1	1.36	6.41	0.35	1.13
S2	0.87	7.41	0.96	1.24
M3	3.36	2.31	1.67	2.58
M4b	2.15	6.92	1.94	3.79
M5b	4.51	33.78	6.84	24.12

Table 7: $Err_{\%}$ for methods for example 2-10D

5.1.3 Membrane model subjected to the displacement of supports -10D case

For 10 variables, the computational cost is higher not only due to the larger size of P but also due to the higher cost of a single simulation caused by the higher complexity of the problem. When the classic method M1 is applied to 10 variables, the rank deficient problems force the use of a higher number of variables $(M-1) \cdot P$ than suggested, which makes this method more computationally expensive for more variables compared to other methods. Table 6 shows the number of points which had to be taken to obtain the full rank matrix in comparison with PC basis size P and recommended [4] size $(M-1) \cdot P$. For order 3 errors of the mean, standard deviation and 95th percentile equal to 3.57%, 8.05%, 0.29%, respectively. Error of the sensitivity index of random variable 4, which together with variable 7 is much higher than the rest of the sensitivity indices, is equal to 2.09%. For the rest of the considered methods a rank deficiency problem does not appear in the cases considered.

Figure 16 shows the results for quasi random sequences (S1 and S2), when $2P$ or $(M-1)P$ points are taken into account. Also in this example S2 outperforms S1 with the exception of the sensitivity index S_4^{Tot} when only $2P$ are taken into account.

The general comparison presented in Table 7, is made with a small number of points equal to $2P$. The method M1 is not presented in this table, because it requires a much higher computational cost due to the rank deficiency problem as mentioned before. The methods combining random and criteria-based approaches as well as the use of quasi-random sequences enable calculations for 10 variables with a much smaller number of points when compared to classic method M1. The quasi random sequences and especially Halton sequence (S2) outperform other methods, thus seem to be a good choice in this example.

5.2 Global sensitivity outcomes

The sensitivity analysis outcomes were analysed in the case of each model to study the influence of uncertainties of given values on the chosen quantities of interest.

variable	E	L_0	H_0	Δ_p
S^{Tot}	0.6460	0.0059	0.0942	0.2746

Table 8: Total sensitivity indices S^{Tot} in cable model - values obtained by MC

method	Mean	Standard deviation	95th percentile
S1	4.51	49.99	10.73
S2	9.09	26.97	0.79
M1 (25 points)	7.75	3.17	4.91
M5b	2.67	2.85	0.62

Table 9: $Err_{\%}$ between solution reduced to 2D and MC 10D solution, $p = 4$, $2P = 30$ regression points

Quantity of interest	R_{max}	u_{max}
p_{ia}	0.9503	0.9222
k_f	0.0514	0.0781
k_{aw}	0.0013	0.0011

Table 10: S^{Tot} in model 3

5.2.1 Cable model

In local sensitivity analysis small changes around the base points are investigated. As shown in [51], in this model the order of importance of variables changes with changes in the base point of Δ_p. When Δ_p is in the range from 0.0065 m to 0.01 m, Δ_p is the dominant value. Whereas for Δ_p near lower limit is almost irrelevant. It also influences values of the coefficients of E and L_0. Therefore, it is interesting to perform on this example global sensitivity analysis to get knowledge of global influence. Table 8 presents total sensitivity indices for each variable. The results confirm that although the variability of H_0 is high when compared to other variables, its contribution to the output variance is very small. However, the smallest is S^{Tot} of L_0, which locally has high sensitivity when Δ_p is small, but its variability was small. Globally, E is the most significant. Despite the small local coefficients for some base points, Δ_p is the second most important parameter. It confirms that abdominal wall behaviour is important to properly predict forces in the fasteners

5.2.2 Membrane model subjected to displacement of supports - Reduction of the 10D model

The sensitivity index values change with orientation of the implant (Fig. 17). However, variables 4 and 7 (with the highest variability) together or individually are always dominant. These variables correspond to the strains of the abdominal wall in the oblique direction. Sensitivity indices of all other variables are in each case lower than 0.03 (sum of all other total sensitivity indices lower than 0.05). Therefore, 10D model can be reduced to 2D problem.

The methods were compared on the reduced to 2D example. Results (for M5b mean) are presented in Table 9. Methods M1, M2, M3 are not considered because the number of combinations of $p + 1$ roots is smaller than $2P$. Therefore, all points are taken into account. The change in variance obtained by the quasi random method (S1, S2) is higher than one could expect from sensitivity indices. Method M5b results in the highest accuracy. Reduction to 2D problems significantly reduces computational costs.

5.3 Model 3 - imposed pressure

The coefficient of variation of R_{max} is equal to 0.22 and of u_{max} 0.1026. In Table 10 total sensitivities are presented. It can be seen that great majority of both output variance is due to uncertainty of the pressure. Elasticity of the foundations could not be treated as a random variable due to its small sensitivity index. The influence of fascia elasticity is also relatively small. These outcomes imply that more detailed studies on intra-abdominal pressure should be conducted.

Although neither abdominal wall nor fascia elasticity uncertainty are important in this model, their influence is high in model 2, where the coefficient of variance is equal to 0.53 and all random variables are related to the abdominal wall mechanics. In future optimisation procedures the number of variables can be reduced in both models according to presented sensitivity index values.

6 Conclusions

We applied the PC method to the implant models used in ventral hernia repair. In these examples we compared different methods of choosing regression points within polynomial chaos expansion. Although the final problem is non-linear, and non-smooth with a high random variable variation, it was possible to obtain sufficient accuracy by the polynomial chaos regression based method.

The best method for choosing the set of points used in the numerical method in our 10D model seems to be a random subset of Hermite roots. However, in examples with a lower number of variables including the reduced model, the method based on a D-optimal choice from a random candidate set drawn by LHS is the most accurate.

The relation between errors and choice of points is highly dependent on the problem studied. In such a case the application of the adaptive method seems to be very reasonable. However, the question is how to choose a criterion which will be effective in our problem. Nevertheless, the presented study can be useful in terms of a decision about the initial set of candidate points for adaptive methods, e.g. error oriented algorithms for design of experiments.

The presented methodology will be used for conducting further studies with the use of implant models in order to draw clinically important conclusions. It will be applied to implants with different mechanical properties and different hernia locations. Also, the methodology will be applied to the much more computationally expensive model of the whole abdominal wall with hernia implant,where the MC model would be computationally infeasable. These types of models in the context of hernia repair are described in [25].

Based on the results obtained so far, employing a probabilistic framework in hernia repair modelling seems to be necessary, e.g. due to underestimation of junction forces by single deterministic calculations performed for the mean values. However, the obstacle is the lack of proper knowledge about the distribution of the random variables and their correlation which is currently based on an insufficiently large number of experiments. The obtained global sensitivity results indicate where priorities in further experimental research should be established.

In model 1 (the cable model) the uncertainty of Young's modulus has the strongest influence on the uncertainty of the horizontal reaction.

In the case of model 2, the uncertainty of the displacement of the supports referring to the strains in oblique direction in the lower part are the most significant. High variability of the strains in the oblique directions results in their having a large influence on the variance of the output. A high variation of abdominal wall elasticity means that the approach taken to ventral hernia repair needs to be patient-specific. A step in this direction can be taken with the use of the non-invasive method of *in vivo* characterization of abdominal wall properties [56]. Nevertheless in the latter methodology variation between sessions with the same subjects was noticed. Therefore, the proposed PC method can be useful also in development of patient-specific methodology.

In the model 3 (subjected to pressure) the sensitivity of the uncertainty to the pressure is much higher than it is to the elasticity of abdominal wall and fascia. Therefore, the studies on intraabdominal pressure in humans during crucial actions like coughing should be enlarged in order to get more detailed information about its distribution.

Future two-criteria [50] optimisation under uncertainty of implant choice due to minimisation of forces and mesh bulging can be performed on reduced models: model subjected to displacement with 2 random variables, model 3 subjected to intra-abdominal pressure with 1 random variable, which will reduce computational cost.

Acknowledgements This work was partially supported by grant UMO-2015/17/N/ST8/02705 from the National Science Centre, Poland, and by the subsidy for the development of young scientists given by the Faculty of Civil and Environmental Engineering, Gdańsk University of Technology. Computations were performed partially in TASK Computer Science Centre, Gdańsk, Poland.

References

1. Acosta Santamaría, V., Siret, O., Badel, P., Guerin, G., Novacek, V., Turquier, F., Avril, S.: Material model calibration from planar tension tests on porcine linea alba. Journal of the Mechanical Behavior of Biomedical Materials **43**, 26–34 (2015). DOI 10.1016/j.jmbbm.2014.12.003
2. de Aguiar, P., Bourguignon, B., Khots, M., Massart, D., Phan-Than-Luu, R.: D-optimal designs. Chemometrics and Intelligent Laboratory Systems **30**(2), 199 – 210 (1995). DOI http://dx.doi.org/10.1016/0169-7439(94)00076-X
3. Antille, G., Weinberg, A., et al.: A Study of D-optimal Designs Efficiency for Polynomial Regression. Université de Genève/Faculté des sciences économiques et sociales (2000)
4. Berveiller, M., Sudret, B., Lemaire, M.: Stochastic finite element: a non intrusive approach by regression. Revue européenne de mécanique numérique **15**(1–3), 81–92 (2006). DOI 10.3166/remn.15.81-92
5. Blatman, G., Sudret, B.: An adaptive algorithm to build up sparse polynomial chaos expansions for stochastic finite element analysis. Probabilistic Engineering Mechanics **25**(2), 183–197 (2010). DOI 10.1016/j.probengmech.2009.10.003

6. Blatman, G., Sudret, B.: Efficient computation of global sensitivity indices using sparse polynomial chaos expansions. Reliability Engineering & System Safety **95**(11), 1216–1229 (2010). DOI 10.1016/j.ress.2010.06.015
7. Blatman, G., Sudret, B.: Adaptive sparse polynomial chaos expansion based on least angle regression. Journal of Computational Physics **230**(6), 2345–2367 (2011)
8. Blatman, G., Sudret, B., Berveiller, M.: Quasi random numbers in stochastic finite element analysis. Mécanique & Industries **8**(3), 289–297 (2007). DOI 10.1051/meca:2007051
9. Breuing, K., Butler, C.E., Ferzoco, S., Franz, M., Hultman, C.S., Kilbridge, J.F., Rosen, M., Silverman, R.P., Vargo, D., Group, V.H.W., et al.: Incisional ventral hernias: review of the literature and recommendations regarding the grading and technique of repair. Surgery **148**(3), 544–558 (2010)
10. Burnaev, E., Panin, I., Sudret, B.: Effective Design for Sobol Indices Estimation Based on Polynomial Chaos Expansions, pp. 165–184. Springer International Publishing, Cham (2016). DOI 10.1007/978-3-319-33395-3_12
11. Carter, S.A., Hicks, S.C., Brahmbhatt, R., Liang, M.K.: Recurrence and pseudorecurrence after laparoscopic ventral hernia repair: predictors and patient-focused outcomes. The American surgeon **80**(2), 138–48 (2014)
12. Chamoin, L., Florentin, E., Pavot, S., Visseq, V.: Robust goal-oriented error estimation based on the constitutive relation error for stochastic problems. Computers & Structures **106-107**(i), 189–195 (2012). DOI 10.1016/j.compstruc.2012.05.002
13. Cho, I., Lee, Y., Ryu, D., Choi, D.H.: Comparison study of sampling methods for computer experiments using various performance measures. Structural and Multidisciplinary Optimization **55**(1), 221–235 (2017). DOI 10.1007/s00158-016-1490-6
14. Choi, S.K., Grandhi, R.V., Canfield, R.A., Pettit, C.L.: Polynomial chaos expansion with latin hypercube sampling for estimating response variability. AIAA journal **42**(6), 1191–1198 (2004)
15. Cobb, W.S., Burns, J.M., Kercher, K.W., Matthews, B.D., Norton, H.J., Heniford, B.T.: Normal intraabdominal pressure in healthy adults. Journal of Surgical Research **129**(2), 231–235 (2005)
16. Cooney, G.M., Lake, S.P., Thompson, D.M., Castile, R.M., Winter, D.C., Simms, C.K.: Uniaxial and biaxial tensile stress–stretch response of human linea alba. Journal of the Mechanical Behavior of Biomedical Materials **63**, 134–140 (2016)
17. Crestaux, T., Le Maître, O., Martinez, J.M.: Polynomial chaos expansion for sensitivity analysis. Reliability Engineering & System Safety **94**(7), 1161 – 1172 (2009). Special Issue on Sensitivity Analysis
18. Deeken, C.R., Thompson, D.M., Castile, R.M., Lake, S.P.: Biaxial analysis of synthetic scaffolds for hernia repair demonstrates variability in mechanical anisotropy, non-linearity and hysteresis. Journal of the mechanical behavior of biomedical materials **38**, 6–16 (2014)
19. Dubourg, V., Sudret, B., Bourinet, J.M.: Reliability-based design optimization using kriging surrogates and subset simulation. Structural and Multidisciplinary Optimization **44**(5), 673–690 (2011). DOI 10.1007/s00158-011-0653-8
20. Fedorov, V.V.: Theory of optimal experiments. Academic Press, INC (english translation) (1972)
21. Filomeno Coelho, R., Lebon, J., Bouillard, P.: Hierarchical stochastic metamodels based on moving least squares and polynomial chaos expansion. Structural and Multidisciplinary Optimization **43**(5), 707–729 (2011). DOI 10.1007/s00158-010-0608-5
22. Fishman, G.S.: Monte Carlo. Springer New York, New York, NY (1996). DOI 10.1007/978-1-4757-2553-7
23. Gao, Z., Zhou, T.: On the choice of design points for least square polynomial approximations with application to uncertainty quantification. Communications in Computational Physics **16**(2), 365–381 (2014). DOI 10.4208/cicp.130813.060214a
24. Ghanem, R.G., Spanos, P.D.: Stochastic Finite Elements: A Spectral Approach. Springer-Verlag (1991)
25. Hernández-Gascón, B., Mena, A., Pena, E., Pascual, G., Bellón, J., Calvo, B.: Understanding the passive mechanical behavior of the human abdominal wall. Annals of biomedical engineering **41**(2), 433–444 (2013)
26. Hernández-Gascón, B., Peña, E., Grasa, J., Pascual, G., Bellón, J.M., Calvo, B.: Mechanical response of the herniated human abdomen to the placement of different prostheses. Journal of biomechanical engineering **135**(5), 051,004 (2013)
27. Hu, C., Youn, B.D.: Adaptive-sparse polynomial chaos expansion for reliability analysis and design of complex engineering systems. Structural and Multidisciplinary Optimization **43**(3), 419–442 (2011). DOI 10.1007/s00158-010-0568-9
28. Huang, X., Liu, Y., Zhang, Y., Zhang, X.: Reliability analysis of structures using stochastic response surface method and saddlepoint approximation. Structural and Multidisciplinary Optimization pp. 1–10 (2016). DOI 10.1007/s00158-016-1617-9
29. Huberts, W., Donders, W., Delhaas, T., Vosse, F.: Applicability of the polynomial chaos expansion method for personalization of a cardiovascular pulse wave propagation model. International Journal for numerical methods in biomedical engineering **30**(12), 1679–1704 (2014)
30. Isukapalli, S.S.: Uncertainty analysis of transport-transformation models. Ph.D. thesis, Graduate School New Brunswick (1999)
31. Junge, K., Klinge, U., Prescher, A., Giboni, P., Niewiera, M., Schumpelick, V.: Elasticity of the anterior abdominal wall and impact for reparation of incisional hernias using mesh implants. Hernia **5**(3), 113–118 (2001)
32. Le Maître, O.P., Knio, O.M.: Spectral Methods for Uncertainty Quantification. Scientific Computation. Springer Netherlands, Dordrecht (2010). DOI 10.1007/978-90-481-3520-2
33. Le Maître, O.P., Reagan, M.T., Najm, H.N., Ghanem, R.G., Knio, O.M.: A stochastic projection method for fluid flow: Ii. random process. Journal of Computational Physics **181**(1), 9 – 44 (2002). DOI http://dx.doi.org/10.1006/jcph.2002.7104
34. Lee, S.H., Chen, W.: A comparative study of uncertainty propagation methods for black-box-type problems. Structural and Multidisciplinary Optimization **37**(3), 239 (2008). DOI 10.1007/s00158-008-0234-7
35. Lubowiecka, I.: Mathematical modelling of implant in an operated hernia for estimation of the repair persistence. Computer methods in biomechanics and biomedical engineering **18**(4), 438–445 (2015)
36. Lubowiecka, I., Szepietowska, K., Szymczak, C., Tomaszewska, A.: Preliminary study on the optimal choice of an implant and its orientation in ventral hernia repair. Journal of Theoretical and Applied Mechanics **54**(2), 411–421 (2016). DOI 10.15632/jtam-pl.54.2.411
37. Lyons, M., Mohan, H., Winter, D., Simms, C.: Biomechanical abdominal wall model applied to hernia repair. British Journal of Surgery **102**(2), e133–e139 (2015)

38. Maurer, M., Röhrnbauer, B., Feola, A., Deprest, J., Mazza, E.: Mechanical biocompatibility of prosthetic meshes: A comprehensive protocol for mechanical characterization. Journal of the mechanical behavior of biomedical materials **40**, 42–58 (2014)
39. McKay, M.D., Beckman, R.J., Conover, W.J.: A comparison of three methods for selecting values of input variables in the analysis of output from a computer code. Technometrics **42**(1), 55–61 (2000)
40. Morokoff, W.J., Caflisch, R.E.: Quasi-Random Sequences and Their Discrepancies. SIAM J. SCl. COMPUT **15**(6), 1251–1279 (1994). DOI 10.1137/0915077
41. Redhe, M., Forsberg, J., Jansson, T., Marklund, P.O., Nilsson, L.: Using the response surface methodology and the d-optimality criterion in crashworthiness related problems. Structural and Multidisciplinary Optimization **24**(3), 185–194 (2002). DOI 10.1007/s00158-002-0228-9
42. Schobi, R., Sudret, B., Wiart, J.: Polynomial-Chaos-based Kriging. International Journal for Uncertainty Quantification **5**(2), 171–193 (2015). DOI 10.1615/Int.J.UncertaintyQuantification.2015012467
43. Simón-Allué, R., Calvo, B., Oberai, A., Barbone, P.: Towards the mechanical characterization of abdominal wall by inverse analysis. Journal of the Mechanical Behavior of Biomedical Materials **66**, 127–137 (2017)
44. Simón-Allué, R., Hernández-Gascón, B., Lèoty, L., Bellón, J., Peña, E., Calvo, B.: Prostheses size dependency of the mechanical response of the herniated human abdomen. Hernia **20**(6), 839–848 (2016)
45. Smith, K.: On the standard deviations of adjusted and interpolated values of an observed polynomial function and its constants and the guidance they give towards a proper choice of the distribution of observations. Biometrika **12**(1-2), 1–85 (1918). DOI 10.1093/biomet/12.1-2.1
46. Sobol, I.M.: Global sensitivity indices for nonlinear mathematical models and their Monte Carlo estimates. Mathematics and Computers in Simulation **55**(1-3), 271–280 (2001). DOI 10.1016/S0378-4754(00)00270-6
47. Song, C., Alijani, A., Frank, T., Hanna, G., Cuschieri, A.: Elasticity of the living abdominal wall in laparoscopic surgery. Journal of biomechanics **39**(3), 587–591 (2006)
48. Sudret, B.: Global sensitivity analysis using polynomial chaos expansions. Reliability Engineering & System Safety **93**(7), 964–979 (2008). DOI 10.1016/j.ress.2007.04.002
49. Suryawanshi, A., Ghosh, D.: Reliability based optimization in aeroelastic stability problems using polynomial chaos based metamodels. Structural and Multidisciplinary Optimization **53**(5), 1069–1080 (2016). DOI 10.1007/s00158-015-1322-0
50. Szymczak, C., Lubowiecka, I., Szepietowska, K., Tomaszewska, A.: Two-criteria optimisation problem for ventral hernia repair. Computer Methods in Biomechanics and Biomedical Engineering **20**(7), 760–769 (2017)
51. Szymczak, C., Lubowiecka, I., Tomaszewska, A., Śmietański, M.: Modeling of the fascia-mesh system and sensitivity analysis of a junction force after a laparascopic ventral hernia repair. Journal of Thoretical and Applied Mechanics **48**(4), 933–950 (2010)
52. Szymczak, C., Lubowiecka, I., Tomaszewska, A., Śmietański, M.: Investigation of abdomen surface deformation due to life excitation: implications for implant selection and orientation in laparoscopic ventral hernia repair. Clinical biomechanics (Bristol, Avon) **27**(2), 105–10 (2012). DOI 10.1016/j.clinbiomech.2011.08.008
53. Szymczak, C., Śmietański, M.: Selected problems of laparoscopic ventral hernia repair - modeling and simulation. alfa-medica press Gdańsk (2012)
54. Tomaszewska, A., Lubowiecka, I., Szymczak, C., Śmietański, M., Meronk, B., Kłosowski, P., Bury, K.: Physical and mathematical modelling of implant-fascia system in order to improve laparoscopic repair of ventral hernia. Clinical Biomechanics **28**(7), 743 – 751 (2013). DOI http://dx.doi.org/10.1016/j.clinbiomech.2013.06.009
55. Tran, D., Mitton, D., Voirin, D., Turquier, F., Beillas, P.: Contribution of the skin, rectus abdominis and their sheaths to the structural response of the abdominal wall ex vivo. Journal of biomechanics **47**(12), 3056–3063 (2014)
56. Tran, D., Podwojewski, F., Beillas, P., Ottenio, M., Voirin, D., Turquier, F., Mitton, D.: Abdominal wall muscle elasticity and abdomen local stiffness on healthy volunteers during various physiological activities. Journal of the mechanical behavior of biomedical materials **60**, 451–459 (2016)
57. Wiener, N.: The homogeneous chaos. American Journal of Mathematics **60**(4), 897–936 (1938)
58. Winkelmann, K., Górski, J.: The use of response surface methodology for reliability estimation of composite engineering structures. Journal of Theoretical and Applied Mechanics **52**(4), 1019–1032 (2014)
59. Xiu, D., Karniadakis, G.E.: The Wiener–Askey Polynomial Chaos for Stochastic Differential Equations. SIAM Journal on Scientific Computing **24**(2), 619–644 (2002). DOI 10.1137/S1064827501387826
60. Zein, S., Colson, B., Glineur, F.: An Efficient Sampling Method for Regression-Based Polynomial Chaos Expansion. Communications in Computational Physics **13**(4), 1173–1188 (2012). DOI 10.4208/cicp.020911.200412a

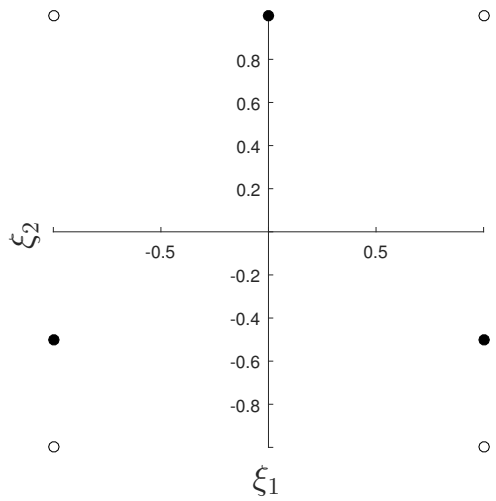

(a) D-optimal points chosen from uniform range from -2 to 2 with a step 0.5 including weight

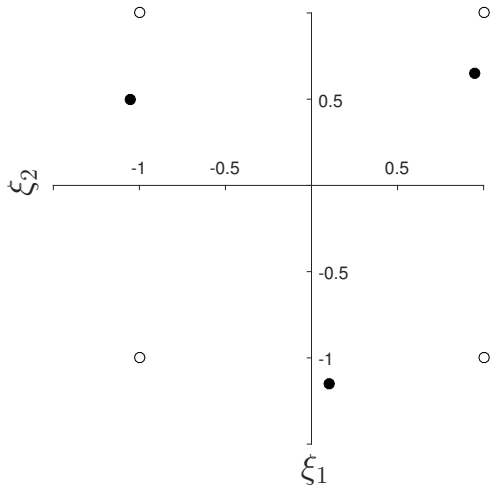

(b) D-optimal points chosen from uniform range from -1.5 to 1.5 with a step 0.05 including weight

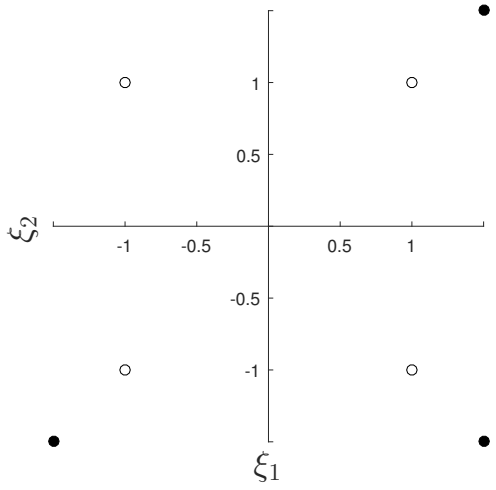

(c) D-optimal points chosen from uniform range from -1.5 to 1.5 with a step 0.05 without weight

Fig. 6: D-optimal points compared to the classic design, Hermite basis ($M = 2$, $p = 1$), black points - chosen points, empty points - classic choice (method M1)

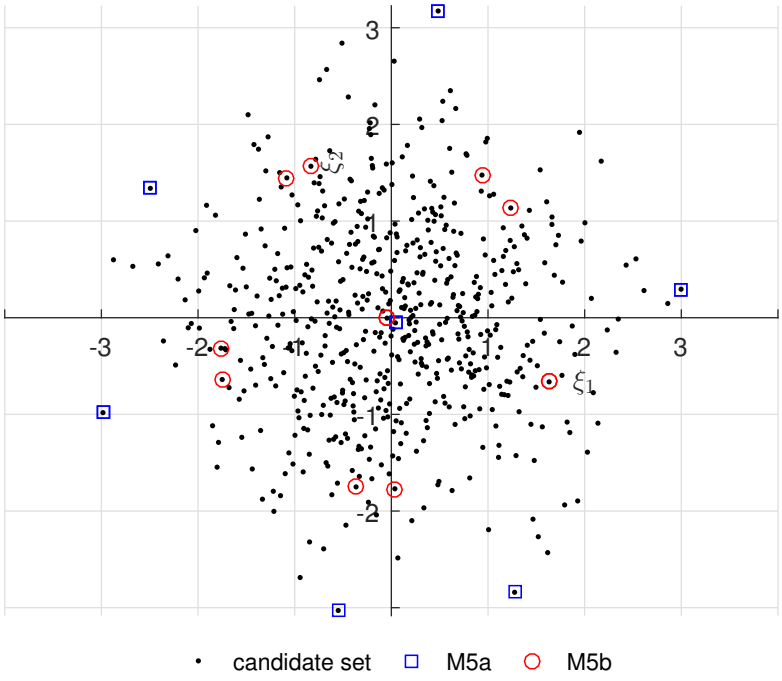

Fig. 7: Example of D-optimal set of points from the candidate set drawn by LHS method when D-optimality is conducted without (M5a) and with weight (M5b), Hermite basis, $M = 2$, $p = 2$

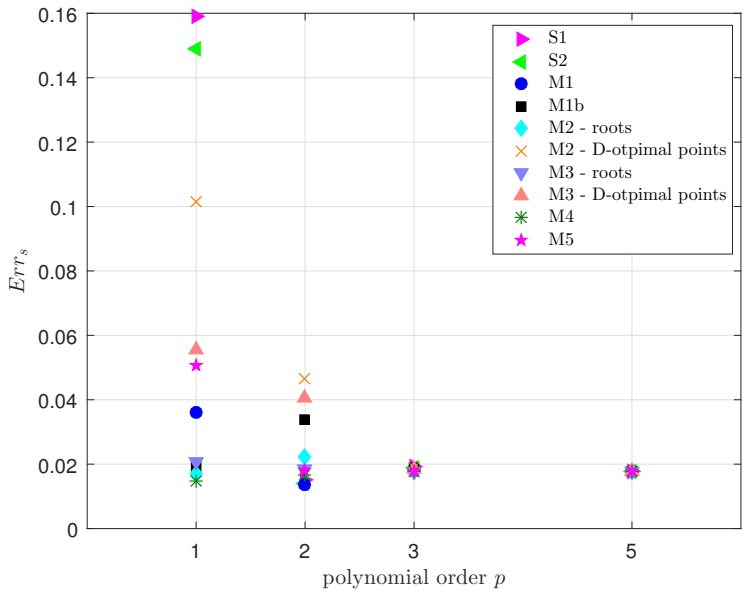

Fig. 8: Err_s obtained for different methods, model 1

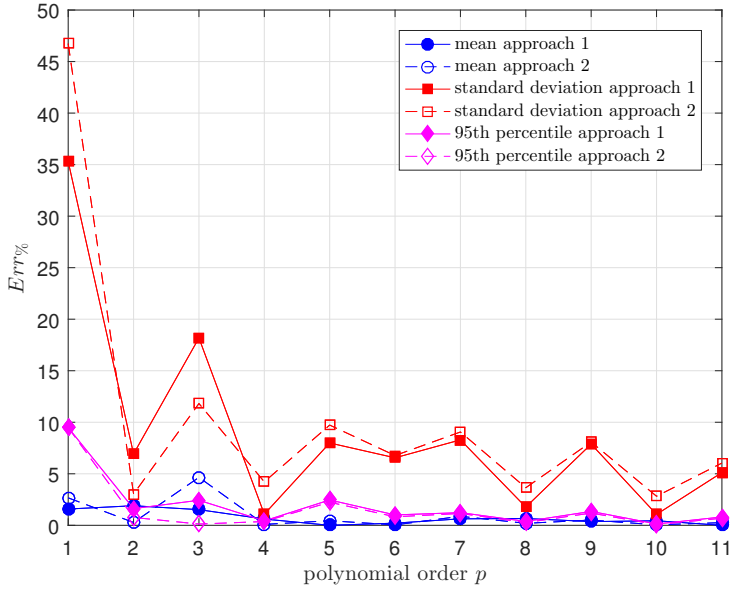

Fig. 9: $Err_{\%}$ of the mean, standard deviation and 95th percentile of the maximum reaction using method M1 using approach 1 (4) and 2 (5)

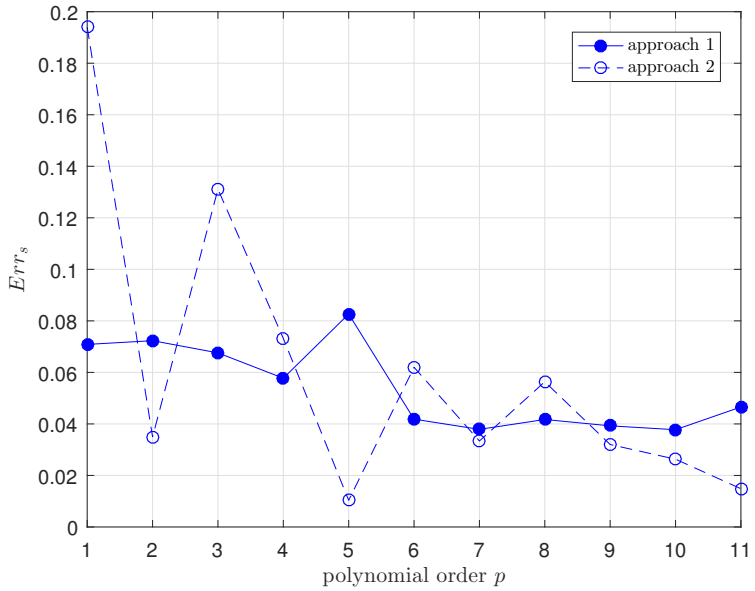

Fig. 10: Err_S obtained by approach 1 (4) and 2 (5) in example 2-3D

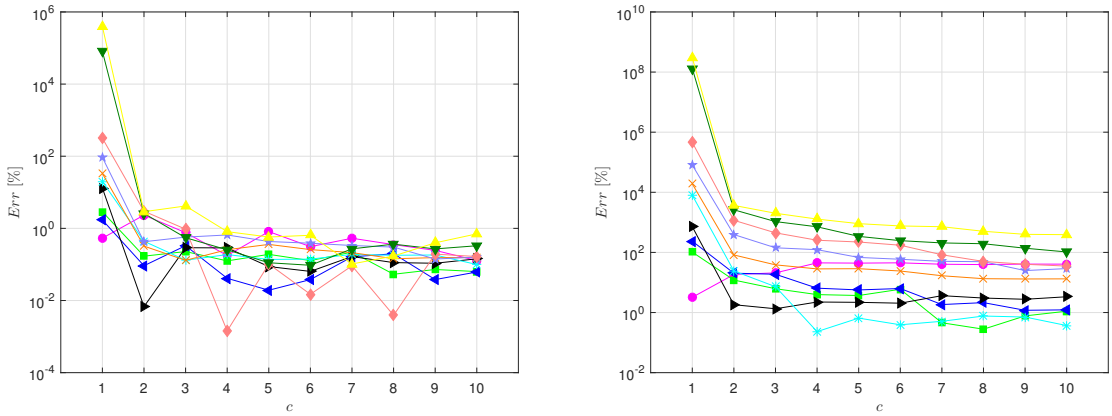

(a) mean

(b) standard deviation

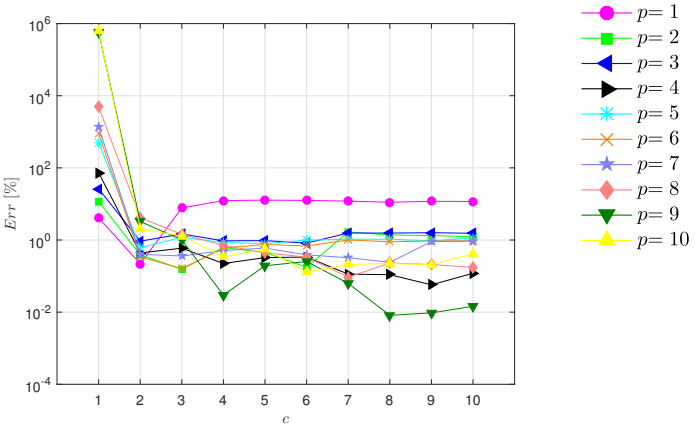

(c) 95th percentile

Fig. 11: Error obtained by method S2 for different orders and a different number of regression points equals $N = c \cdot P$, example 2-3D

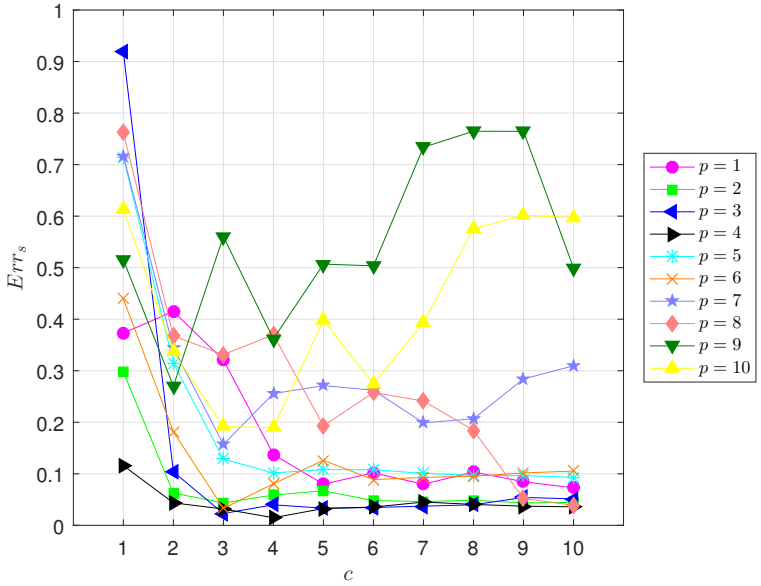

Fig. 12: Err_s obtained by method S2 for different orders and a different number of regression points equals $N = c \cdot P$, example 3-3D

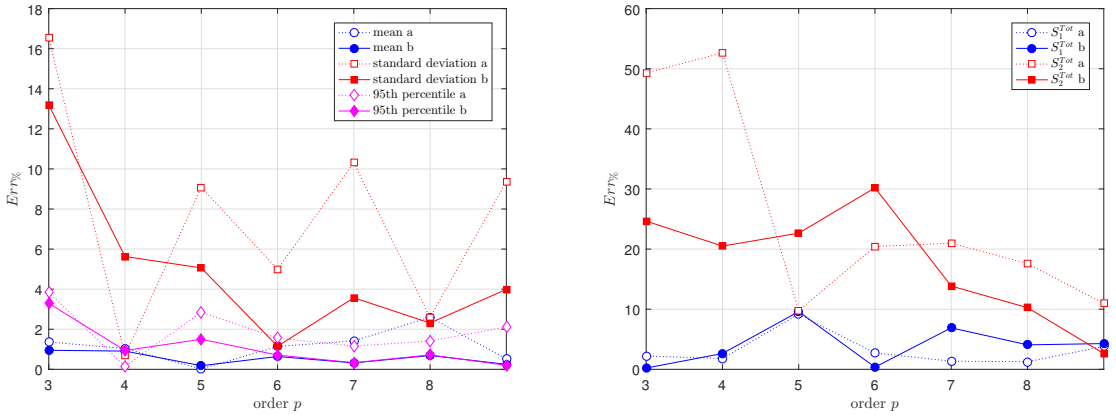

(a) mean, standard deviation, 95th percentile

(b) sensitivity indices

Fig. 13: Err_s, when method M2 was applied in variants without (a) and with (b) weight for different orders, example 2-3D)

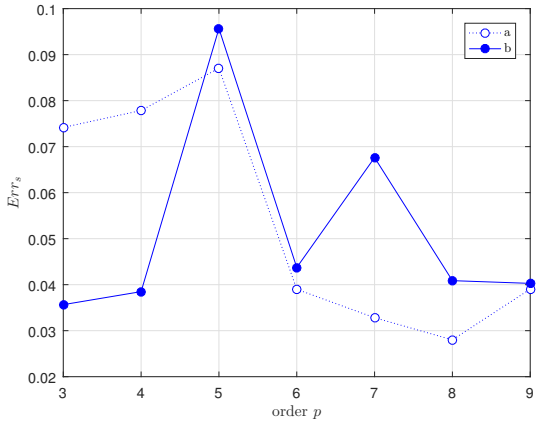

Fig. 14: Err_s obtained by method M2 , example 2-3D

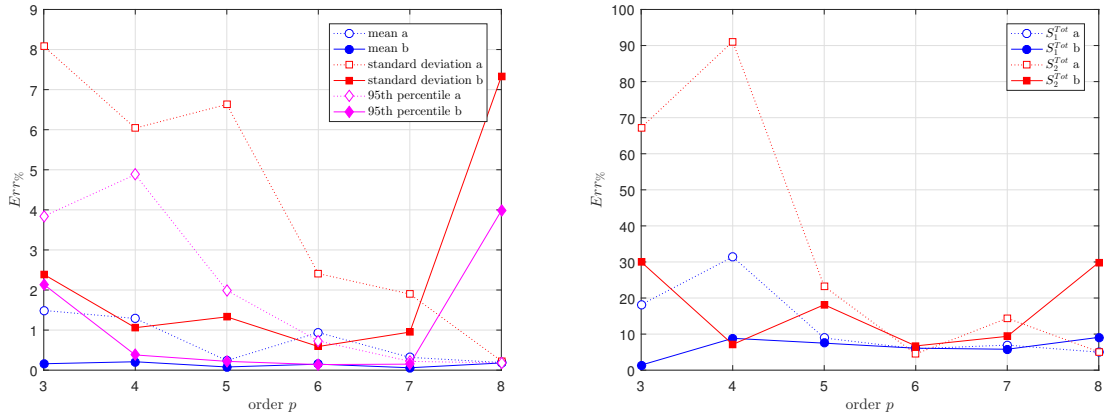

(a) mean, standard deviation, 95th percentile

(b) sensitivity indices

Fig. 15: Err_s, when method M5 was applied in variant without (a) and with (b) weight for different orders (mean result from a couple of drawn LHS candidate sets of points, example 2-3D)

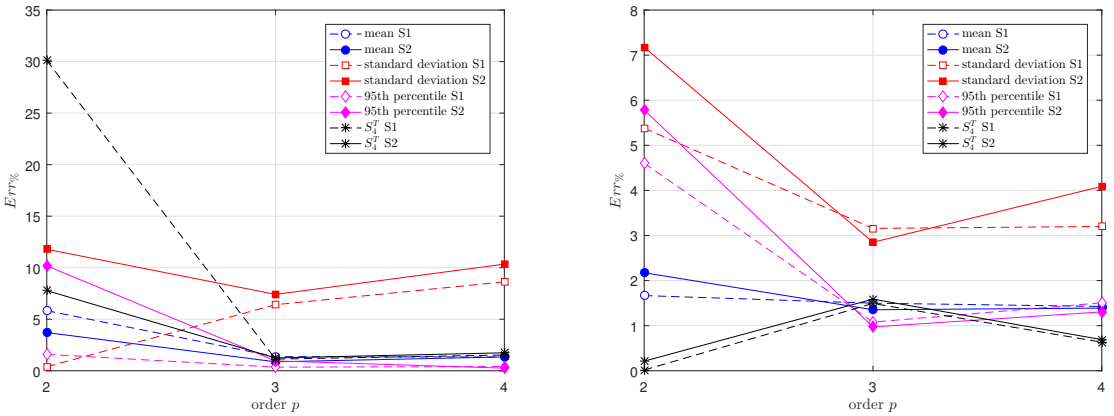

(a) $2P$ points

(b) $(M-1)P$ points

Fig. 16: $Err_{\%}$, when method S1 and S2 is applied, example 2-10D

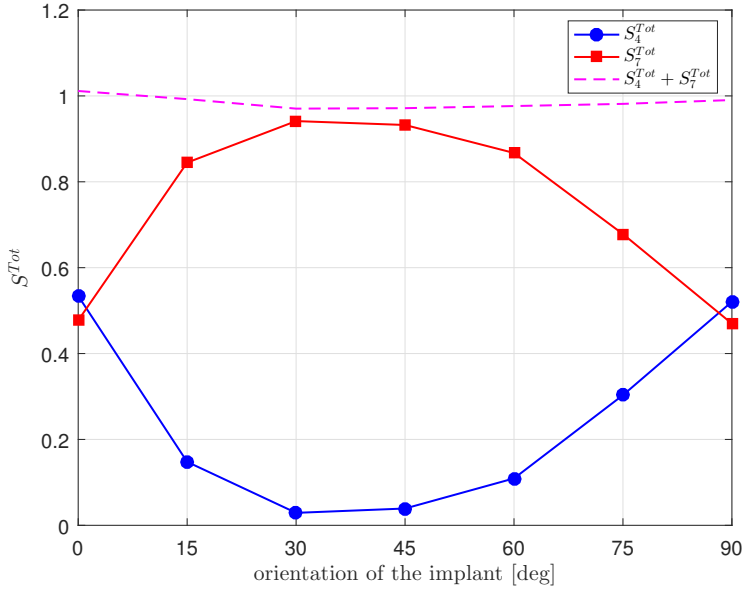

Fig. 17: S^{Tot} obtained for different orientations of implant, example 2-10D